THE ASTROPHYSICAL JOURNAL, 438:385–393, 1995 January 1

ECLIPSE TIMINGS OF THE LOW-MASS X-RAY BINARY EXO 0748−676: STATISTICAL ARGUMENTS AGAINST ORBITAL PERIOD CHANGES

PAUL HERTZ AND KENT S. WOOD
E. O. Hulburt Center for Space Research, Naval Research Laboratory, Code 7621, Washington, DC 20375-5352;
hertz@xip.nrl.navy.mil, wood@xip.nrl.navy.mil

AND

LYNN COMINSKY[1]
Department of Physics and Astronomy, Sonoma State University, Rohnert Park, CA 94928;
lynnc@charmian.sonoma.edu
Received 1994 April 15; accepted 1994 July 5

ABSTRACT

EXO 0748−676, an eclipsing low-mass X-ray binary, is one of only about four or five low-mass X-ray binaries for which oribital period evolution has been reported. We observed a single eclipse egress with *ROSAT*. The time of this egress is consistent with the apparent increase in P_{orb} previously reported on the basis of *EXOSAT* and *Ginga* observations. Standard analysis, in which $O-C$ (observed minus calculated) timing residuals are examined for deviations from a constant period, implicitly assume that the only uncertainty in each residual is measurement error and that these errors are independent.

We argue that the variable eclipse durations and profiles observed in EXO 0748−676 imply that there is an additional source of uncertainty in timing measurements, that this uncertainty is intrinsic to the binary system, and that it is correlated from observation to observation with a variance which increases as a function of the number of binary cycles between observations. This intrinsic variability gives rise to spurious trends in $O-C$ residuals which are misinterpreted as changes in the orbital period.

We describe several statistical tests which can be used to test for the presence of intrinsic variability. We apply those statistical tests which are suitable to the EXO 0748−676 observations. The apparent changes in the orbital period of EXO 0748−676 can be completely accounted for by intrinsic variability with an rms variability of $\sim$0.35 s per orbital cycle. The variability appears to be correlated from cycle-to-cycle on timescales of less than 1 yr. We suggest that the intrinsic variability is related to slow changes in either the source's X-ray luminosity or the structure of the companion star's atmosphere. We note that several other X-ray binaries and cataclysmic variables have previously reported orbital period changes which may also be due to intrinsic variability rather than orbital period evolution.

Subject headings: binaries: eclipsing — stars: individual (EXO 0748−676) — X-rays: stars

1. INTRODUCTION

Low-mass X-ray binaries (LMXBs) are among the brightest Galactic X-ray sources. They are powered by the accretion of matter from a Roche-lobe filling, low-mass companion onto a neutron star primary (Lewin & Joss 1983; White et al. 1994). The accretion may be driven by the loss of angular momentum through gravitational radiation or magnetic braking or by the nuclear evolution of the secondary star (Bhattacharya & van den Heuvel 1991; Verbunt 1993; Verbunt & van den Heuvel 1994). Each model makes specific predictions for the evolution of the LMXB. For conservative mass transfer from a Roche lobe filling secondary star obeying a mass radius relation $R_2 \propto M_2^n$

$$\frac{\dot{P}_{orb}}{P_{orb}} = \left(\frac{3}{2}n - \frac{1}{2}\right)\frac{\dot{M}_2}{M_2} \qquad (1)$$

(Verbunt 1990; Bhattacharya & van den Heuvel 1991). For a main-sequence secondary ($n \simeq 1$), the loss of angular momentum causes the orbit to shrink, so P_{orb} decreases and $\dot{P}_{orb} < 0$. If P_{orb} were to increase in this case, then the secondary star would cease to fill its Roche lobe and accretion would stop. For a degenerate secondary ($n < 0$), mass loss causes the degenerate star to expand. The orbit will grow to accommodate the larger Roche lobe, P_{orb} will increase, and $\dot{P}_{orb} > 0$. For LMXBs with main-sequence secondaries, equation (1) and observed accretion rates of $-\dot{M}_2 \simeq 10^{-10}$–$10^{-8}\ M_\odot\ \mathrm{yr}^{-1}$ imply that the timescale for evolution of the orbital period, $\tau_{orb} \equiv |P_{orb}/\dot{P}_{orb}|$, is expected to be approximately 10^8 to 10^{10} yr for a 1 $M_\odot$ secondary.

The sign and magnitude of the orbital period derivative $\dot{P}_{orb}$ are arguably the most critical diagnostics of LMXB evolution. However only about four or five LMXBs have measured orbital period derivatives, and in each of these there are problems rectifying the measured τ_{orb} with theory (Tavani 1991; White et al. 1994). In 4U 1822−37, the 5.6 hr orbital period is increasing on a timescale of 2.9×10^6 yr (Hellier et al. 1990) where a decreasing P_{orb} is expected. The ultracompact binary 4U 1820−30, which has a 685 s orbital period and a degenerate white dwarf secondary, is expected to have its orbital period increase with a timescale of $\gtrsim 1.1 \times 10^7$ yr (Verbunt 1987; Rappaport et al. 1987). However, the orbital period of 4U 1820−30 is observed to decrease with $\tau_{orb} \simeq 1.9 \times 10^7$ yr (van der Klis et al. 1993b; see also van der Klis et al. 1993a, Tan et al. 1991; Sansom et al. 1989). The 40.8 hr orbital period

[1] Visiting Professor, Stanford Linear Accelerator Center.

of the pulsar Her X-1 is decreasing on a timescale of 7.6×10^7 yr (Deeter et al. 91), which is larger than can be explained by the observed accretion rate. The 4.8 hr X-ray binary Cyg X-3, which may or may not be a LMXB (van Kerkwijk et al. 1992), exhibits an increasing orbital period ($\tau_{orb} \simeq 7.3 \times 10^5$ yr) with possible evidence for a measurable second period derivative (Kitamoto et al. 1992; van der Klis & Bonnet-Bidaud 1989). The observed period evolution in Cyg X-3 may be consistent with nonconservative mass loss through a stellar wind (Tavani 1991; van Kerkwijk et al. 1992).

The eclipsing LMXB EXO 0748−676 shows 8.3 minute duration eclipses that recur every 3.82 hr (Parmar et al. 1986). The sharp-edged eclipse transitions (duration of ingress/egress $\lesssim 40$ s) provide good fiducial markers for timing the orbital period P_{orb}. Eclipses and eclipse transitions have been observed with *EXOSAT* and *Ginga*, and the $O-C$ residuals (observed minus calculated residuals are the delay in eclipse time over that expected for a constant period system) have been used to determine the evolution of the orbital period (Parmar et al. 1991; Asai et al. 1992). The 39 eclipses observed between 1985 February 15 and 1991 August 23 cannot be fitted with a constant period nor with a constant period derivative; the introduction of a sinusoidally varying P_{orb} provides an acceptable fit (Asai et al. 1992). This behavior can be interpreted as providing evidence for a third body in the system which orbits the inner X-ray binary with a ~ 12 yr period.

Third bodies have been proposed to account for apparently sinusoidal variations in the $O-C$ residuals of a number of close binary systems, including RS CVn systems (Van Buren 1986), W UMa systems (Havnes 1980), cataclysmic variables (Warner 1988), and X-ray binaries. However the variations in the $O-C$ residuals track changes in the orbital period only if any remaining variability, after accounting for orbital period changes, is a white-noise process such as measurement error. In the case of EXO 0748−676, the time of eclipse is determined by observing eclipse ingress, eclipse egress, and eclipse duration. The time of an event which is fixed in the binary system, such as conjunction (or mid-eclipse) is then estimated from these measurements. The observation that all of these events vary in duration indicates that none of the four contacts represent a fixed point in the system. If the variation in the time and duration of eclipse ingress and egress is correlated from one cycle to the next, then the $O-C$ residuals do not represent changes in the orbital period, but rather represent such changes plus a stochastic term related to the accumulated variability in the timing of eclipse features (Lombard & Koen 1993).

We show that the observational evidence is consistent with the assumption that eclipse timings in EXO 0748−676 show a correlation from cycle to cycle. These correlations may be due to changes in the secondary star's atmosphere, which acts as the occulting edge during eclipses, and these changes are long lived compared to the orbital period of the system. Under the assumption that eclipse timings vary stochastically but nonindependently from eclipse to eclipse, we use several statistical tests to show that the available timing evidence is consistent with no orbital period evolution. That is, all of the observed $O-C$ residuals can be accounted for by stochastic changes in the eclipse light curve and there is no need to invoke either period evolution or a third body.

In this paper we briefly discuss our *ROSAT* observation (§ 2); other than confirming the general trend of the most recent timings from *Ginga*, the lack of a fully observed eclipse makes this observation of limited use in our analysis. We thus rely on published eclipse timings from *EXOSAT* and *Ginga*. In § 3 we discuss the reasons for believing that there may be stochastic but correlated changes in the observed orbital period. We present the statistical formalism for interpreting these variations in apparent P_{orb} in § 4. Here we also develop and apply several statistical tests showing that the available data are consistent with this interpretation, and that a third body is not required to explain the $O-C$ residuals. Finally (§ 5) we briefly discuss physical mechanisms which may be the cause of the variations in eclipse duration, and thus give rise to the spurious variability in the $O-C$ diagram.

2. *ROSAT* TIMINGS OF EXO 0748−676

EXO 0748−676 was observed three times with the *ROSAT* Position Sensitive Proportional Counter (PSPC; Trümper 1983; Pfeffermann et al. 1986) during the AO1 and AO2 phases of the mission. The source was detected during 23 observing intervals ranging in duration from 464 to 3238 s; a total of 30.6 ks of live time was obtained on target. On 1991 November 11, EXO 0748−676 was in eclipse at the beginning of one observing interval. Several minutes later, eclipse egress was observed; only a partial eclipse was observed. Using the cycle numbering scheme of Parmar et al. (1991), this is the egress from eclipse 15440. A light curve of this observation is shown in Figure 1.

The PSPC window support structure is opaque to X-rays. In order to prevent the support structure shadow from being imaged, the normal operating mode of *ROSAT* includes a slow "wobble" ($\pm 3'$ in 400 s of time). Timing observations of point shources should be taken off-axis, where the point spread function is sufficiently broad that the window support structure is no longer sharply imaged. Unfortunately, observations of EXO 0748−676 were obtained with the target on axis. The effect of the spacecraft wobble is seen clearly in the post-egress light curve of EXO 0748−676 (Fig. 1).

Eclipse egress occurs near a minimum in the "wobbled" light curve. This makes it difficult to determine the exact time of the beginning of eclipse egress and impossible to determine the time of the end of eclipse egress. We have estimated the beginning of eclipse egress with an uncertainty of ± 5 s. We then correct this time to the solar system barycenter using the

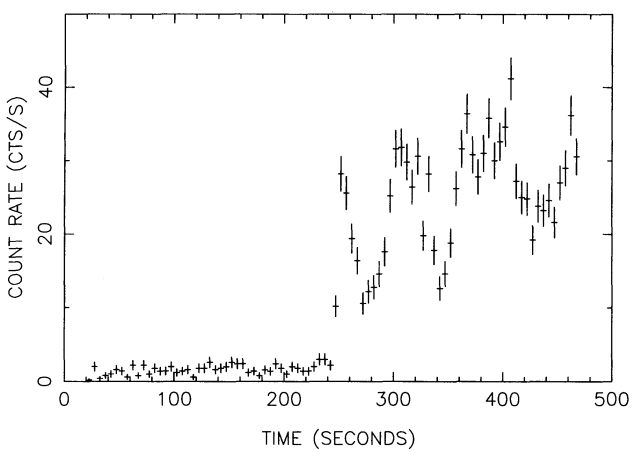

FIG. 1.—The light curve of EXO 0748−676 observed with *ROSAT* on 1991 November 11. The observation begins during eclipse, and eclipse egress is clearly visible. The quasi-periodic variations in the posteclipse flux are due to window support structures occulting the source as the spacecraft wobbles.

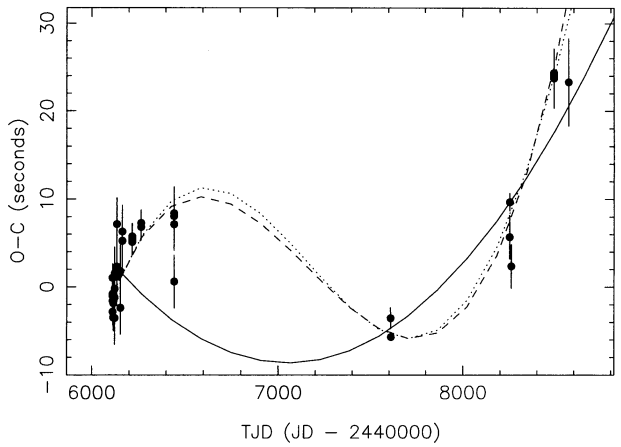

FIG. 2.—The $O-C$ residuals for EXO 0748−676 from the combined *EXOSAT/Ginga/ROSAT* data set. The residuals are relative to a constant period. The best-fitted quadratic (*solid*), cubic (*dashed*), and sinusoidal (*dotted*) ephemerides are shown. Data are from Parmar et al. (1991), Asai et al. (1992), and the current paper.

timcor routines of the *ROSAT* analysis package PROS 2.1 (Conroy et al. 1993; Manning et al. 1993). We find that the beginning of eclipse egress for eclipse 15440 occurs at barycentric TJD 8571.752298 ± 0.000058.

The complete eclipses observed with *EXOSAT* and *Ginga* ranged between 484.4 and 501.4 s in duration, with an average of 492.7 s and a standard deviation of 4.8 s (Parmar et al. 1991; Asai et al. 1992). We can therefore *estimate* that mid-eclipse for eclipse 15440 occurred at approximately barycentric TJD 8571.749447 ± 0.000080. The residual time delays for all observed eclipses are plotted in Figure 2 after subtracting the best-fit constant period ephemeris for T_n, the time of mid-eclipse n,

$$T_n = T_0 + nP_{\rm orb}\,, \tag{2}$$

where

$$T_0 = 6111.574555 \pm 0.000004 \text{ (barycentric TJD)} \tag{3a}$$

$$P_{\rm orb} = 0^{\rm d}.1593377334 \pm 0^{\rm d}.0000000005 \tag{3b}$$

The *ROSAT* eclipse continues the trend of increasing residuals observed with the most recent *Ginga* timings. We have also plotted the best quadratic (constant $\dot{P}_{\rm orb}$), cubic (constant $\ddot{P}_{\rm orb}$), and sinusoidal fits to the $O-C$ residuals. Since the *ROSAT* point has such a large error bar, we obtain essentially the same parameters for the fitted functions as Asai et al. (1992) did. Additional eclipse timings have been obtained by the *ASCA* satellite (Corbet et al. 1994).

3. PHYSICAL EVIDENCE FOR CORRELATED ECLIPSE TIMINGS

As we will show in § 4, if the $O-C$ residuals are not independent, then the standard analysis of $O-C$ plots, in which the $O-C$ data are least-squares fitted to parametric functions of cycle number, is invalid. The *EXOSAT* and *Ginga* observations of eclipses in EXO 0748−676 (Parmar et al. 1991; Asai et al. 1992) indicate in several ways that such correlations are present in the eclipse timings.

First, the eclipse durations ($\Delta T_{\rm ecl}$) and ingress/egress durations ($\Delta T_{\rm ing}$, $\Delta T_{\rm egr}$) vary from eclipse to eclipse. We have already noted that $\Delta T_{\rm ecl}$ of the 33 eclipses observed in full ranges between 492.7 and 501.4 s. During 30 eclipses observed with *EXOSAT*, $\Delta T_{\rm ing}$ and $\Delta T_{\rm egr}$ range between 1.5 and 39.9 s. The uncertainty on these three duration measurements is only a few seconds ($\lesssim 3$ s). Finally we note that $\Delta T_{\rm ing}$ and $\Delta T_{\rm egr}$ are only loosely correlated (Fig. 3). For ~50% of the observed eclipses, $\Delta T_{\rm ing} \simeq \Delta T_{\rm egr}$; however, of the other 50% of the eclipses, there is no correlation between the two durations.

The eclipses are caused by the secondary occulting the neutron star. As the line-of-sight to the neutron star passes through the secondary's atmosphere and any additional circumstellar material, absorption effects give rise to the gradual ingress and egress (Parmar et al. 1986, 1991; Asai et al. 1992). The changing eclipse duration and ingress/egress durations are one indication that changes in the structure of the occulting material are occurring. An independent indication is the variability of the optical light curve for UY Vol, the optical counterpart of EXO 0748−676. Correlations between the X-ray state of EXO 0748−676 and the magnitude, color, and shape of its optical light curve have been noted by several observers, as have cycle-to-cycle variability in the optical light curve shape (Schmidtke & Cowley 1987; van Paradijs et al. 1988; Motch et al. 1989; Schoembs & Zoeschinger 1990; Thomas et al. 1993).

X-ray heating of the surface of the companion star is the cause for at least some of the optical variability observed. Parmar et al. (1991) suggest several physical mechanisms which might give rise to detectable effects on X-ray eclipse timing, including flows on the surface of the secondary which are driven by X-ray heating, flaring activity on the secondary, and the formation of an X-ray induced evaporative wind or corona about the secondary. All of these effects can be asymmetrical, that is give rise to different changes in eclipse timings for ingress and egress. The first effect, X-ray–induced surface flows, might give rise to changes in eclipse duration of a few seconds (Parmar et al. 1991)—this is marginally consistent with the range of observed $\Delta T_{\rm ecl}$ but not the observed ranges of $\Delta T_{\rm ing}$ and $\Delta T_{\rm egr}$. The latter two effects may give rise to changes in both the scale height of the atmosphere as well as the accretion rate through the Roche lobe, and thus the X-ray luminosity.

All three effects thus might indicate a correlation between X-ray luminosity and eclipse timing changes. Such an effect was noted by Parmar et al. (1991): there is a tendency for the

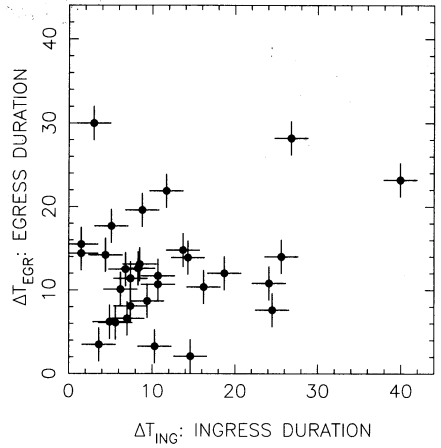

FIG. 3.—Scatter diagram of the duration of eclipse egress $\Delta T_{\rm egr}$ vs. the duration of eclipse ingress $\Delta T_{\rm ing}$ as measured by *EXOSAT* (Parmar et al. 1991). For about half of the observed eclipses $\Delta T_{\rm egr} \simeq \Delta T_{\rm ing}$; for the other half there is no correlation.

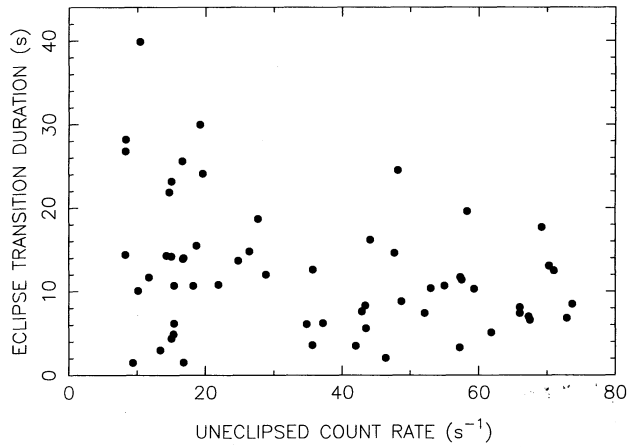

FIG. 4a

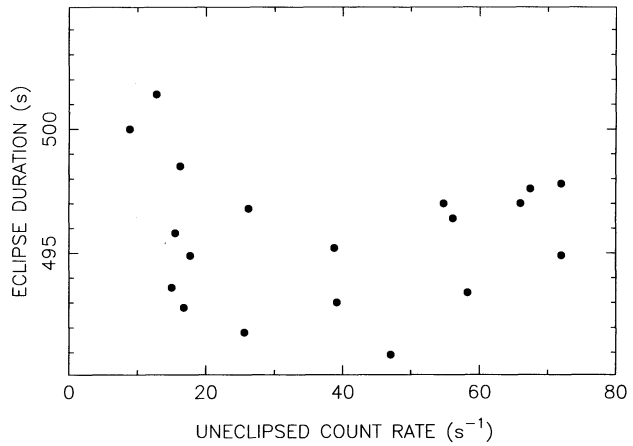

FIG. 4b

FIG. 4.—(*a*) Scatter diagram of duration of eclipse egress and ingress (ΔT_{egr}, ΔT_{ing}) vs. observed X-ray flux. There is a weak correlation with longer eclipse transitions occurring when the source is less bright. (*b*) Scatter diagram of duration of eclipse (ΔT_{ecl}) vs. observed X-ray flux. There is a no correlation. Data are from *EXOSAT* observations (Parmar et al. 1991).

longer duration ingress and egress transitions to occur when the observed uneclipsed X-ray flux is low (Fig. 4*a*). A Spearman rank order test shows that transition time and uneclipsed flux are anticorrelated at the 93% confidence level. We might expect eclipse duration ΔT_{ecl} and uneclipsed X-ray flux to be correlated (Fig. 4*b*), but a Spearman rank order test shows no significant correlation.

What we are most interested in here are correlations between eclipses. Parmar et al. (1986) noted that the X-ray flux of EXO 0748−676 tends to remain at the same level for extended periods of time. In Figure 5 we show the uneclipsed X-ray flux of EXO 0748−676 as a function of cycle number. The slowly varying trend in X-ray flux is clearly visible. A Spearman rank order test shows that the uneclipsed flux is correlated with the flux of the previous observation at the 99.98% (3.9 σ) confidence level. Weaker correlations are detected between ΔT_{ecl} (92% confidence level) and ΔT_{egr} (96% confidence level) in one eclipse and the previously observed eclipse, but no significant correlation is observed in ΔT_{ing}. Therefore if the X-ray flux gives rise to changes in the eclipse timing, then the observed times of eclipses will change slowly as a function of X-ray flux over long periods of time. These correlations invalidate the standard analysis of $O-C$ residuals.

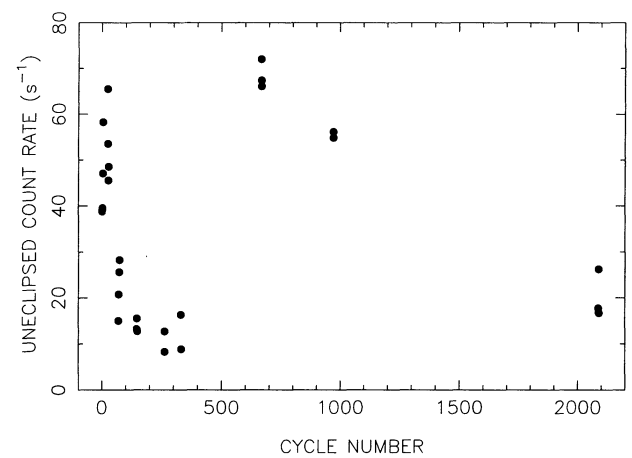

FIG. 5.—The observed X-ray flux of EXO 0748−676 as a function of time, as measured in orbital cycles. Note that, except for the earliest observations, the source tends to remain at a given X-ray flux for extended periods of time. Data are from *EXOSAT* observations (Parmar et al. 1991).

4. STATISTICAL EVIDENCE FOR CORRELATED ECLIPSE TIMINGS

4.1. *General Statistical Methods*

Let T_n be the time of mid-eclipse for cycle number n. If the only uncertainty in the measurement of T_n is measurement error, then

$$T_n = F(n) + e_n , \tag{4}$$

where $F(n)$ is the predicted time of eclipse n from the ephemeris and e_n are independent identically distributed measurement errors with variance s_e^2. The $O-C$ residuals are

$$R_n = T_n - F(n) . \tag{5}$$

The standard analysis in § 2 and Figure 2, as well as that used by Parmar et al. (1991) and Asai et al. (1992), involves adjusting the parameters of the ephemeris $F(n)$ so as to minimize the sum of the squares of the residuals. If the assumptions above are true, then $R_n = e_n$, the residuals are independent and identically distributed random variables, the sum of the squares of the residuals is distributed as a χ^2 random variable, and the assumptions involved in the standard least-squares analysis are correct.

However, if there is an additional term of uncertainty in the measurement of T_n which is intrinsic to the binary system, such as asymmetric changes in the eclipse transitions, then the instantaneous period measured for cycle n is

$$\begin{aligned} D_n &= T_n - T_{n-1} \\ &= F(n) - F(n-1) + \varepsilon_n , \end{aligned} \tag{6}$$

where ε_n is the additional intrinsic uncertainty in cycle n. Now we have

$$\begin{aligned} T_n &= T_0 + \sum_{i=1}^{n} D_i + e_n \\ &= F(n) + \sum_{i=1}^{n} \varepsilon_i + e_n \end{aligned} \tag{7}$$

and

$$R_n = \sum_{i=1}^{n} \varepsilon_i + e_n \tag{8}$$

(Lacy 1973; Lombard 1995; Koen & Lombard 1993). The $O-C$ residuals R_n are no longer independent. Even with the correct ephemeris $F(n)$, they are no longer distributed like the measurement error, and in particular, one no longer expects R_n to have mean 0 and variance s_e^2. Instead the R_n execute a random walk controlled by the (essentially) stochastic process $\{\varepsilon_i\}$ (Lombard & Koen 1993). The tendency of random walk processes to move away from their mean, in this case the true ephemeris, and then return is well known. The random walk process is nonstationary and the variance of the $O-C$ residuals increases linearly with n (Lacy 1973; see below). This nonstationarity means that determining changes in the period P from the $O-C$ diagram is complicated. If the wandering of the $O-C$ residuals is fit, then one can fit quadratics as the process moves away from the mean and sinusoids when it has begun to move back. The period of the sinusoid is typically greater than the interval over which the eclipses have been observed.

When every cycle is observed, then the statistics of the random variable R_n have been worked out in great detail in a branch of statistics called "Cumulative Sum Statistics' or "Cusum Tests" (Woodward & Goldsmith 1964; van Dobben de Bruyn 1968; Lombard & Koen 1993). Cusum tests were developed to monitor the quality of manufactured products and the deviation of products from a desired norm. If the "product" that one monitors is the binary period of a stellar system, then cusum tests can be used to search for changes and trends in that period.

Several statistical tests have been proposed to detect deviations in observed period from an assumed constant period when every period is observed. For each test, the null hypothesis assumed is that the period is constant and the additional intrinsic uncertainty ε_i in each cycle has a zero expectation value and a constant variance ($E(\varepsilon_i) = 0$ and $\mathrm{Var}(\varepsilon_i) = \sigma_\varepsilon^2 < \infty$). The $O-C$ residual R_n for cycle n is the cumulative sum

$$R_n = \sum_{i=1}^{n} \varepsilon_i \tag{9}$$

if we ignore measurement errors.

In the excursion test (Page 1955; Johnson & Bagshaw 1974), the test statistic V_n is the maximum excursion in the $O-C$ residuals through cycle n,

$$V_n = \max_{k \le n} \{R_k - \min_{i \le k} R_i\} . \tag{10}$$

The distribution of $V_n/(n\sigma_\varepsilon)^{1/2}$ in the limit $n \to \infty$ is known (Johnson & Bagshaw 1974). In this test, one determines whether the largest observed excursion V_n is significantly larger than zero; if so, then the null hypothesis is rejected and one of the assumptions in the null hypothesis (constant P, independent ε_i) is invalid.

The span test of Isles & Shaw (1987; see also Lombard 1995) uses the largest $O-C$ residual as the test statistic, but the size of the residual is measured in units of the standard deviation of the N observed cycle lengths,

$$s = \sqrt{\frac{\sum_{i=1}^{N}(D_i - P)^2}{N-1}} . \tag{11}$$

The test statistic for the span test is $S = \max_{i \le N} R_n/s$ and the distribution of S is given by Williamson (1985). Once again, if the value of the test statistic S is significantly larger than zero, the null hypothesis is rejected.

In the contingency test of Sterne & Campbell (1937; see also Lacy 1973), a two-dimensional contingency table is constructed where the nominal variables are both binary valued. One is whether the cycle length D_n exceeds the (assumed) constant period P, and the other is whether cycle n occurs in the first half or the second half of the data series of length N. See Table 1.

In Table 1, the marginal quantities A_1 and A_2 are the totals in each row, B_1 and B_2 are the totals in each column, and C is the grand total for the table. Under the null hypothesis, the value of

$$\chi_c^2 = \sum_{i,j} \frac{(a_{ij} - A_i B_j/C)^2}{A_i B_j/C} \tag{12}$$

should be distributed as a χ^2 variable with one degree of freedom. If χ_c^2 exceeds a critical value, then the null hypothesis is rejected.

The excursion and span tests can be used only when every cycle is observed. When cycles are missed, the critical value of the test statistic might be either larger (because the variance of the statistic is greater) or smaller (because the largest excursions of R_n might have been missed) than described above. In the contingency test, only consecutive cycles can be included in the contingency table; other observations are not used. These tests have been used to search for period changes in Mira and other semiregular variables (Sterne & Campbell 1937; Lacy 1973; Isles & Saw 1987; Percy et al. 1990; Koen 1992), where the bright, long-period nature of these stars makes it possible to collect data sets in which every minimum (or maximum) is observed. When cycles are missed, which is typical of short period binary systems such as cataclysmic variables or LMXBs, the distribution of the test statistics cannot be determined. In general, the distribution of the test statistics will depend on the pattern of missed cycles.

In the case of missed cycles, such as the available eclipse timings for EXO 0748−676, statistical tests can take advantage of the fact that the variance of the residuals increases with the number of cycles observed. Lombard (1995) looks at the power spectrum of the cycle lengths D_n. For data with missing cycles, the power spectrum must be estimated using a periodogram (Lomb 1976; Scargle 1982) or related technique. The

TABLE 1

FORMAT FOR CONTINGENCY TABLE IN STERNE AND CAMPBELL CONTINGENCY TEST

D_n	$n \le N/2$	$n > N/2$	Total
$D_n > P$	a_{11}	a_{12}	A_1
$D_n \le P$	a_{21}	a_{22}	A_2
Total.....	B_1	B_2	C

NOTE.—The data series spans N cycles where D_n is the length of cycle n and P is the trial constant period. The table entries (a_{11}, a_{12}, a_{21}, a_{22}) are the number of cycle lengths D_n which either do ($D_n > P$) or do not ($D_n \le P$) exceed the trial period P and which either do ($n \le N/2$) or do not ($n > N/2$) fall in the first half of the time spanned by the data series. The marginal quantities are the totals for each row (A_1, A_2), for each column (B_1, B_2), or the grand total (C).

power spectrum is the sum of the power spectra from the period variation, the measurement errors, and the additional uncertainty ε (which Lombard calls intrinsic error). If the period is constant, then the only term which contributes to the power spectrum at zero frequency is ε. If there is significant power at zero frequency, it is due either to a changing period or intrinsic error. In practice, it is difficult to estimate the needed power because of long-term trends in the data. The data set needs to be dense enough to allow determination of the periodogram as well.

Eddington & Plakidis (1929) noted that the difference in the $O-C$ residuals is a function of the number of cycles between the observations. From equation (8),

$$R_{n+m} - R_n = \sum_{i=n+1}^{n+m} \varepsilon_i + e_{n+m} - e_n \,. \tag{13}$$

The difference between two $O-C$ residuals is the sum of m uncorrelated fluctuations ε_i and two uncorrelated measurement errors e_i. Recall that σ_ε is the rms variability of the additional intrinsic fluctuations and s_e is the rms variability of the measurements. Define $\bar{u}_m$ to be the expected standard deviation about zero of the difference in $O-C$ residuals over a span of m cycles. Then

$$\begin{aligned} \bar{u}_m &= \sqrt{E[(R_{n+m} - R_n)^2]} \\ &= \sqrt{m\sigma_\varepsilon^2 + 2s_e^2} \,. \end{aligned} \tag{14}$$

If m is an appreciable fraction of the total number of cycles spanned by the data set N, then a correcting factor is needed and

$$\bar{u}_m = \sqrt{m\sigma_\varepsilon^2(1 - m/N) + 2s_e^2} \tag{15}$$

(Eddington & Plakidis 1929). One can then calculate $\bar{u}_m$ as a function of m from the observed $O-C$ residuals and fit it to equation (14) or (15); a best-fitted parameter σ_ε which is significantly different from zero can be taken as statistical evidence of additional intrinsic uncertainty in the cycle length.

4.2. *Statistical Tests on EXO 0748−676 for Correlation*

We wish to test our adopted null hypothesis, that the observed EXO 0748−676 eclipse timings are consistent with a constant period and additional intrinsic variability in the observed timings. Only a small subset of the tests described in § 4.1 can be applied to the EXO 0748−676 eclipse timings. There are 40 eclipse timings in the combined *EXOSAT*/*Ginga*/*ROSAT* data base; thus there are only 39 measurements of the period between eclipse timings. Of these, 24 measure the period between consecutive eclipses (21 by *EXOSAT*, three by *Ginga*). The excursion and span tests cannot be used due to the fact that only 39 residuals were observed over 15,439 cycles of the binary system. The series of eclipse timings is too sparsely populated to estimate the power spectrum, so Lombard's method cannot be applied.

We applied the contingency test to the 24 pairs of consecutive eclipses observed. The mean period observed over $N = 15{,}439$ cycles of the data set is $P = 0.159337753 \pm 0.000000005$ d. If we fill in the contingency table given in Table 1 with the EXO 0748−676 data, we obtain Table 2. Equation (12) yields $\chi_c^2 = 2.9$. This is only significant at the 91% confidence level, so we accept the null hypothesis. We note that, due to the very small number of consecutively observed eclipses by *Ginga*, this is a very weak test when applied to the EXO 0748−676 data.

TABLE 2

STERNE & CAMPBELL CONTINGENCY TABLE FOR EXO 0748−676

D_n	$n \le 7719$	$n > 7719$	Total
$D_n > 0.159337753$	11	0	11
$D_n \le 0.159337753$	10	3	13
Total	21	3	24

NOTE.—The contingency table format is described in Table 1. For EXO 0748−676, there are 24 pairs of consecutive eclipses observed, the data span $N = 15{,}439$ cycles and we adopt the mean period $P = 0.159337753$ days as the trial constant period.

The Eddington & Plakidis (1929) correlative test is the best test for detecting the presence of additional intrinsic uncertainty in the eclipse timings. Since the series of $O-C$ residuals is a random walk process, the expected scatter of $R_{n+m} - R_n$ is an increasing function of m (see eqs. [14] and [15]). For a first cut on showing this, we looked only at the 39 gaps between the 40 eclipse timings. We grouped these into those gaps which cover one cycle (24 instances), these covering 2–99 cycles (seven instances), and those covering ≥ 100 cycles (eight instances). In Table 3 we show that the scatter in the residual differences, $R_{n+m} - R_n$, is an increasing function of the number of cycles in the gap between observations. This is consistent with our null hypothesis.

There are 780 pairs of $O-C$ residuals between the 40 eclipse timings in the EXO 0748−676 data set, with between 1 and 15,439 cycles between observations. We can use these pairs to apply the correlative test to the EXO 0748−676 data. We have grouped the 780 pairs into ~ 60 sets of residual pairs. There are between two and 54 pairs in each set, with ~ 20 being a typical amount, and all the pairs in each set have approximately the same number of cycles between the timings in the pair. In Figure 6 we show $\bar{u}_m$, the scatter in residual differences with m cycles between the measurements, as a function of m. The vertical error bars are the statistical uncertainties in the scatter determinations and are based on propagated measurement errors. The dotted line shows the expected function (eq. [15]) with the measurement uncertainty $s_e = 1.8$ s per measurement and the additional intrinsic uncertainty $\sigma_\varepsilon = 0.35$ s per cycle. The 0.35 s intrinsic uncertainty cannot be detected in single eclipse timings because the measurement error is so much larger, but can only be seen when allowed to accumulate (in a random walk fashion) over thousands of binary periods.

The drawn curve in Figure 6 is not a fit, but merely a visual estimate. The reason formal fitting failed is that there is very poor agreement between the plotted data at short gap lengths ($m \lesssim 2500$) and the expected curve. This is probably due to correlations in the additional intrinsic uncertainty for short timescales (2500 cycles is ~ 1.1 yr). We have already shown

TABLE 3

SCATTER IN RESIDUAL DIFFERENCES AS A FUNCTION OF GAP LENGTH

m Cycles	Number	Mean (s)	Scatter (s)
1	24	−0.3	0.3
2–99	7	−0.3	1.3
≥100	8	1.2	3.2

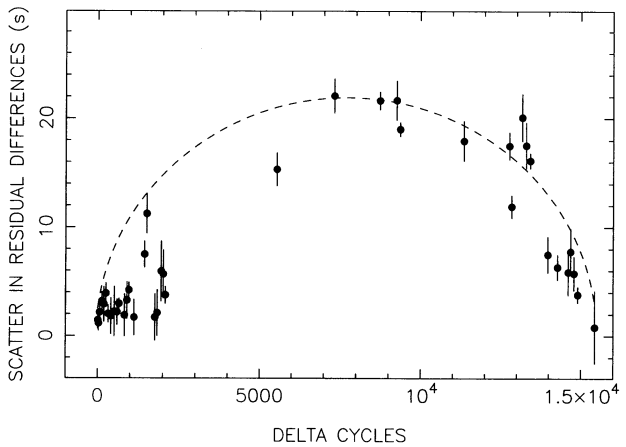

FIG. 6.—The scatter in the differences in $O-C$ residuals $\bar{u}_m$ between observations separated by m orbital cycles as a function of m. The dotted line is the relationship predicted for $\sigma_\epsilon^2 = 0.35$ s per cycle of intrinsic variability and $s_e^2 = 1.8$ s measurement errors. The error bars drawn are statistical only and are generated by propagating measurement errors. We have not plotted bins with large statistical errors due to averaging of small numbers—only data points representing the average of more than five differences have been plotted.

evidence for such correlations in § 3, and the correlative test is completely consistent with that evidence. From this correlation we might infer that changes in the atmosphere of the companion star which affect eclipse timing persist on yearly timescales.

We can test whether the difference in $O-C$ residuals is consistent with the distribution predicted by the correlative test (eq. [13]) using a simple Kolmogorov-Smirnov test. Specifically we test whether the data are consistent with $R_m - R_n$ being drawn from a Gaussian distribution with zero mean and variance $(m-n)\sigma_\epsilon^2 + e_m^2 + e_n^2$. We have calculated the K-S probabilities as a function of the intrinsic uncertainty σ_ϵ for the 39 pairs of consecutive observations of eclipse timings, and the result is shown in Figure 7. A large value of the K-S probability, say exceeding 10%, indicates that the data are consistent with having been drawn from the proposed distribution. The observed EXO 0748−676 data are statistically consistent with

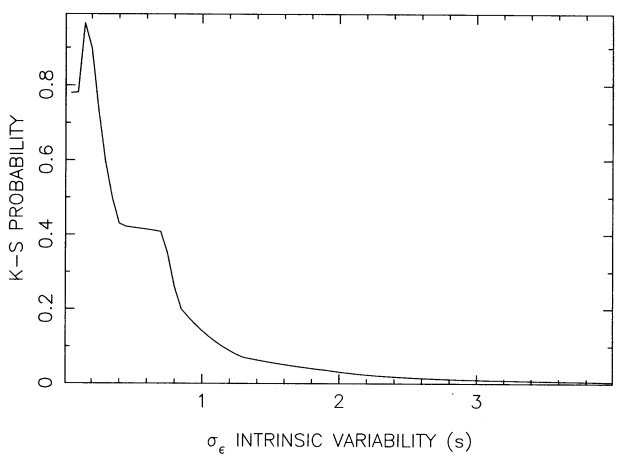

FIG. 7.—A Kolmogorov-Smirnov test is applied to the difference in $O-C$ residuals between consecutive observations. The data are tested for consistency with the residuals being due to meausurement error plus intrinsic variability. The probability that the data are drawn from the tested distribution is plotted as a function of the intrinsic variability per binary cycle. Note that the data are consistent with intrinsic variability of less than 1 s per binary cycle.

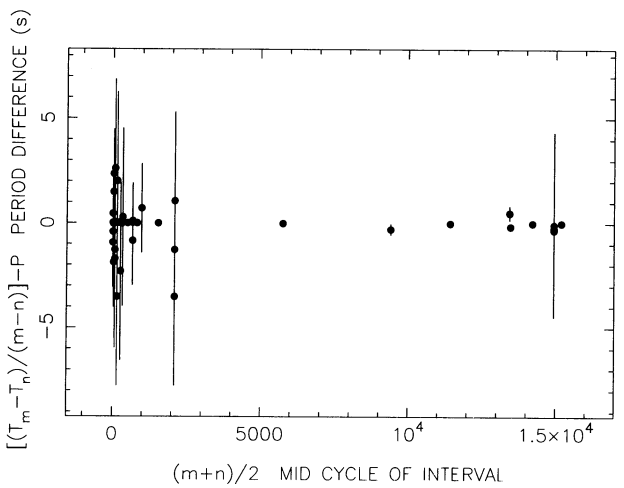

FIG. 8.—The mean period $(T_m - T_n)/(m-n)$ between observations as a function of orbital cycle $(m+n)/2$ during which the measurement was made. There is no apparent change in orbital period.

the differences in $O-C$ residuals being due to intrinsic variability, and the value of that variability σ_ϵ is less than ~ 1 s per binary cycle.

Finally, we might consider how best to fit for a period derivative $\dot{P}$ in the presence of intrinsic uncertainty. Figure 8 shows a plot of the mean periods $(T_m - T_n)/(m-n)$ as a function of $(m+n)/2$ for the 39 pairs of consecutive observations. The errors are the measurement uncertainties. There is no visual evidence for a change in period. If there is a small change in period present, so that $F(n) = T_0 + nP_0 + \frac{1}{2}n^2 P_0 \dot{P}$, then equation (7) implies

$$T_m = T_n = (m-n)\left(P_0 + P_0 \dot{P}\,\frac{m+n}{2}\right) + \left(\sum_{i=n+1}^{m} \epsilon_i + e_m - e_n\right) \qquad (16)$$

(Lombard 1995). This has the form of a linear regression, where the last term acts like a measurement error (Fig. 8). Unfortunately the "error terms" are not independent, since consecutive observations are correlated, so least-squares fitting is not valid for determining $\dot{P}$.

5. DISCUSSION

As we reviewed in § 4.1, there is a body of statistical tests which are designed to detect the presence of intrinsic variability in $O-C$ residuals from periodic stars. These have been applied predominantly to long-period variable stars as they require essentially complete sets of period timings. In these stars, the periodic clock is not kinematic so it is more straightforward to propose physical mechanisms which explain the intrinsic variability.

Applying the same formalism to short period eclipsing binaries like EXO 0748−676 runs into two difficulties. The observed eclipse series are extremely sparse. There is an average of 396 cycles between observed eclipses in the combined *EXOSAT/Ginga/ROSAT* data set. If the 24 pairs of consecutively observed eclipses are excluded, we find that the average waiting period between non-consecutive eclipses is over 1000 cycles. The statistical tests which have been most well developed are not suited for data sets of this sort. Nonetheless we have used the Eddington & Plakidis (1929) correla-

tive test to show that the growth in variance between observed eclipses, as a function of the waiting period between the observed eclipses is consistent with the assumption that it is due to intrinsic varibility, and that this intrinsic variability has a variance of ~ 0.35 s per binary cycle. However, a poor fit for waiting periods less than ~ 2500 cycles (~ 1 yr) implies that the intrinsic variability for cycle to cycle may be correlated on timescales shorter than 1 yr. When the proper variables are regressed against one another (eq. [16] there is no evidence for a nonzero period derivative.

Of course, the most difficult task is to explain where the intrinsic variability comes from. Certainly the binary period is not changing in a stochastic fashion. Rather, the fiducial markers in the binary system which we use to measure eclipse transitions must be moving about in a random manner. There is direct evidence for this in the observed variability of eclipse durations and transitions. The fact that the durations of eclipse ingress and egress do not always correlate well indicates that eclipse timings could be early or late, depending on whether ingress or egress is larger for that eclipse.

The occulting edge for eclipses in EXO 0748−676 is the atmosphere of the companion star. Some fraction of the optical emission from UY Vol, the optical counterpart of EXO 0748−676, comes from the surface of the companion star. Most of the optical emission is due to reprocessed X-rays. Observed variability in the optical light curves of UY Vol, both from cycle-to-cycle and as a function of X-ray luminosity, provides additional evidence that the surface of the companion star undergoes both stochastic and correlated changes.

Several physical mechanisms have been proposed which can give rise to changes in the structure and height of the companion's atmosphere. These physical changes, in turn, affect the relative timing of mid-eclipse in the binary systems revolving coordinate system. Among the mechanisms suggested are X-ray illumination of the companion star changing the structure of its atmosphere (Parmar et al. 1991) or even exciting mass loss (Asai et al. 1992). In support of this general idea, we have noted (weak) correlations between observed X-ray flux and eclipse, egress, and ingress durations, and between X-ray flux and the shape of the optical light curve. We also note that the X-ray flux remains constant for extended periods of time; this may be related to the apparent correlation in the intrinsic variability on shorter timescales.

EXO 0748−676 is not the only short-period binary in which apparent changes in the binary orbital period might be due to intrinsic variability. Van der Klis et al. (1994) have suggested that the apparent evolution of the orbital period in 4U 1820−30 is due to changes in the shape of the X-ray light curve causing the observed orbital phase to appear to drift. Similar changes were proposed to explain changes in the orbital period of Cyg X-3 (van der Klis & Bonnet-Bidaud 1989). Light curve changes are a form of intrinsic variability; if the light curve changes smoothly then the phase of maximum light will be correlated from cycle to cycle and the above methods will be applicable.

There are a large number of cataclysmic variables (CVs) in which long-term sinusoidal variations in the orbital period are proposed based on observations lasting between 0.5 and 1.7 times the proposed long-period cycle. These CVs included U Gem (18 yr, 1 cycle; see Eason et al. 1983 and Beuermann & Pakull 1984), IP Peg (5 yr, 1.5 cycles; Wolf et al. 1993), RW Tri (8 or 14 yr, 0.5 or 1 cycle; Africano et al. 1978), DQ Her (14 yr, 1.7 cycles; Patterson et al. 1978), UX UMa (29 yr, 1.5 cycles; Mandel 1965 and Quigley & Africano 1978), EX Hyd (20 yr, 1.3 cycles; Bond & Freeth 1988). All of these systems have been observed for fewer than 2 cycles. Even the best ephemerides cannot fit all of the observations, and residuals as large as tens of seconds are observed in some of these CVs. The sinsuoidal variations in cataclysmic variables are variously interpreted as due to the presence of a third body, loss of angular momentum from the system, exchange of orbital and spin angular momentum, apsidal motion, and motion of the "hot spot" relative to the two stars. It is conceivable, perhaps even likely, that some of these CVs also show intrinsic variability in their observed periods.

Intrinsic variability in eclipse timings may account for the majority of short-period, compact binaries which show evidence for orbital period evolution. Occam's Razor requires us to consider this hypothesis as an alternative to the presence of a third body in these systems. Unfortunately there are no powerful statistical tools currently available which are well suited for the sparse data that is common with short-period systems. One can always wait—the $O-C$ residuals will eventually diverge from any fitted ephemeris if intrinsic variability is causing apparent changes in the orbital period. In EXO 0748−676 such evidence should become available with current and future observations using the *ASCA* (current) and *XTE* (1995 launch) satellites and the USA instrument onboard the *ARGOS* satellite (1996 launch).

We thank Yin Ly for analysis of the *ROSAT* observations. This work is partially supported by the Office of Naval Research (P. H., K. S. W.), by the NASA *ROSAT* Guest Investigator Program (P. H., K. S. W., L. C.), and by the Department of Energy for work done at SLAC under contract DE-AC03-76SF00515 (LC).

REFERENCES

Africano, J. L., Nather, R. E., Patterson, J., Robinson, E. L., & Warner, B. 1978, PASP, 90, 568
Asai, K., Dotani, T., Nagasa, F., Corbet, R. H. D., & Shaham, J. 1992, PASJ, 44, 633
Beuermann, K., & Pakull, M. W. 1984, A&A, 136, 250
Bhaatacharya, D., & van den Heuvel, E. P. J. 1991, Phys. Rep., 203, 1
Bond, I. A., & Freeth, R. V. 1988, MNRAS, 232, 753
Conroy, M. A., DePonte, J., Moran, J. F., Orszak, J. S., Roberts, W. P., & Schmidt, D. 1993, in ASP Conf. Ser., Vol. 52, Astronomical Data Analysis Software and Systems II, ed. R. J. Hanisch, R. J. V. Brissenden, & J. Barnes (San Francisco: ASP), 238
Corbet, R. H. D., et al. 1994, ApJ, submitted
Deeter, J. E., Boynton, P. E., Miyamoto, S., Kitamoto, S., Nagase, F., & Kawai, N. 1991, ApJ, 383, 324
Eason, E. L. E., Africano, J. L., Klimke, A., Quigley, R. J., Rogers, W., & Worden, S. P. 1983, PASP, 95, 58
Eddington, A. S., & Plakidis, S. 1929, MNRAS, 90, 65
Havnes, O. 1980, A&A, 92, 151
Hellier, C., Mason, K. O., Smale, A. P., & Kilkenny, D. 1990, MNRAS, 244, 39P
Isles, J. E., & Saw, D. R. B. 1987, J. Brit. Astron. Assoc., 97, 106
Johnson, R. A., & Bagshaw, M. 1974, Technometrics, 16, 103
Kitamoto, S., Mizobuchi, S., Yamashita, K., & Nakamura, H. 1992, ApJ, 384, 263
Koen, C. J. 1992, in ASP Conf. Ser., Vol. 30, Variable Stars and Galaxies, ed. B. Warner (San Francisco: ASP), 127
Koen, C., & Lombard, F. 1993, MNRAS, 263, 287
Lacy, C. H. 1973, AJ, 78, 90
Lewin, W. H. G., & Joss, P. C. 1983, in Accretion-driven Stellar X-Ray Sources, ed. W. H. G. Lewin & E. P. J. van den Heuvel (Cambridge: Cambridge Univ. Press), 41
Lomb, N. R. 1976, Ap&SS, 39, 447
Lombard, F. 1995, in Applications of Time Series Analysis in Astronomy and Meteorology, ed. T. Subba Rao (London: Chapman-Hall), in press

Lombard, F., & Koen, C. 1993, MNRAS, 263, 309
Mandel, O. 1965, Perem. Zvezdy, 15, 474
Manning, K. R., Conroy, M. A., DePonte, J., Moran, J. F., Primini, F. A., & Seward, F. D. in ASP Conf. Ser., Vol. 52, Astronomical Data Analysis Software and Systems II, ed. R. J. Hanisch, R. J. V. Brissenden, & J. Barnes (San Francisco: ASP) 484
Motch, C., Pederson, H., Ilovaisky, S. A., Chevalier, C., & Mouchet, M. 1989, in Proc. 23d ESLAB Symp., X-Ray Binaries, ed. J. Hunt & B. Battrick, ESA SP-296, 1, 545
Page, E. S. 1955, Biometrika, 42, 523
Parmar, A. N., Smale, A. P., Verbunt, F., & Corbet, R. H. D. 1991, ApJ, 366, 253
Parmar, A. N., White, N. E., Giommi, P., & Gottwald, M. 1986, ApJ, 308, 199
Patterson, J., Robinson, E. L., & Nather, R. E. 1978, ApJ, 224, 570
Percy, J. R., Colivas, T., Sloan, W. B., & Mattei, J. A. 1990, in ASP Conf. Ser., Vol. 11, Confrontation between Stellar Pulsation and Evolution, ed. C. Cacciari & G. Clementini (San Francisco: ASP), 446
Pfeffermann, E., et al. 1986, Proc. SPIE, Vol. 733, Soft X-ray Optics and Technology, 519
Quigley, R., & Africano, J. 1978, PASP, 90, 445
Rappaport, S., Nelson, L. A., Joss, P. C., & Ma, C.-P. 1987, ApJ, 322, 842
Sansom, A. E., Watson, M. G., Makishima, K., & Dotani, T. 1989, PASJ, 41, 591
Scargle, J. D. 1982, ApJ, 263, 835
Schmidtke, P. C., & Cowley, A. P. 1987, AJ, 92, 374
Schoembs, R., & Zoeschinger, G. 1990, A&A, 227, 105
Sterne, T. E., & Campbell, L. 1937, Ann. Harvard Coll. Obs. 105, 459
Tan, J., Morgan, E., Lewin, W. H. G., Penninx, W., van der Klis, J., van Paradijs, J., Makishima, K., Inoue, H., Dotani, T., & Mitsuda, K. 1991, ApJ, 374, 291
Tavani, M. 1991, Nature, 351, 39
Thomas, B., Corbet, R., Augesteijn, T., Callanan, P., & Smale, A. P. 1993, ApJ, 408, 651
Trümper, J. 1983, Advances in Space Research, 2(4), 241
Van Buren, D. 1986, AJ, 92, 136
van der Klis, M., & Bonnet-Bidaud, J. M. 1989, A&A, 214, 203
van der Klis, M., et al. 1993a, MNRAS, 260, 686
van der Klis, M., Hasinger, G., Verbunt, F., van Paradijs, J., Belloni, T., & Lewin, W. H. G. 1993b, A&A, 279, L21
van Dobbyn de Bruyn, C. S. 1968, Cumulative Sum Tests: Theory and Practice, Griffin Statistical Monograph No. 24 (London: Griffin)
van Kerkwijk, et al. 1992, Nature, 355, 703
van Paradijs, J., van der Klis, M., & Pedersen, H. 1988, A&AS, 76, 185
Verbunt, F. 1987, ApJ, 312, L23
———. 1990, in Neutron Stars and Their Birth Events, ed. W. Kundt (Dordrecht: Kluwer), 179
———. 1993, ARA&A, 31, 93
Verbunt, F., & van den Heuvel, E. P. J. 1994, in X-Ray Binaries, ed. W. H. G. Lewin, J. van Paradijs, & E. P. J. van den Heuvel (Cambridge: Cambridge Univ. Press), in press
Warner, B. 1988, Nature, 336, 129
White, N. E., Nagase, F., & Parmar, A. N. 1994, in X-Ray Binaries, ed. W. H. G. Lewin, J. van Paradijs, & E. P. J. van den Heuvel (Cambridge: Cambridge Univ. Press), in press
Williamson, R. J. 1985, Statistician, 34, 345
Wolf, S., Mantel, K. H., Horne, K., Barwig, H., Schoembs, R., & Baernbantner, O. 1993, A&A, 273, 160
Woodward, R. H., & Goldsmith, P. L. 1964, Cumulative Sum Techniques (Edinburgh: Oliver & Boyd)